Linearity Challenges of LTE-Advanced Mobile Transmitters: Requirements and Potential Solutions

Adnan Kiayani, *Member, IEEE,* Vesa Lehtinen, *Member, IEEE,* Lauri Anttila, *Member, IEEE,* Toni Lähteensuo, and Mikko Valkama, *Senior Member, IEEE*

Abstract

In order to provide higher data rates and to improve radio spectrum utilization, 3GPP has introduced the concept of carrier aggregation (CA) in its Release 10 and onwards, commonly known as LTE-Advanced standard. The CA technology, in particular when applied in a noncontiguous manner, poses serious design and implementation challenges for radio transceivers, mainly due to the allowed flexibility in the transmitted signal characteristics and the nonlinear radio frequency (RF) components in the transmitter (TX) and receiver (RX) chains. As a consequence, substantial nonlinear distortion may occur that not only degrades the transmitted signal quality but can also affect the concurrent operation of the coexisting receiver, when operating in the frequency division duplex (FDD) mode. In this article, the key technical design challenges in terms of linearity requirements for LTE-Advanced mobile terminals are reviewed, and the corresponding self-interference problem related to the potential desensitization of the device's own receiver is highlighted. Then, technical solutions to mitigate the self-interference at the RX band due to a nonlinear power amplifier (PA) in the transmitter chain are reviewed, with specific emphasis on digital self-interference cancellation methods. As demonstrated through simulation and actual RF measurement examples, the cancellation solutions can substantially mitigate the RX desensitization problem, thus relaxing the RF isolation requirements between the TX and RX chains. Such cancellation methods are one potential enabling technique towards the full exploitation of the fragmented RF spectrum and the CA technology in future LTE-Advanced and beyond mobile networks.

Index Terms

Carrier aggregation, digital cancellation, emission requirements, LTE-Advanced, mobile device, nonlinear distortion, power amplifier, RX desensitization, spurious emissions, unwanted emissions.

I. Introduction

Carrier Aggregation (CA) is one of the key features of the Third Generation Partnership Project (3GPP) Long Term Evolution (LTE)-Advanced networks to meet or even surpass the peak data rate targets for the International Mobile

Adnan Kiayani, Vesa Lehtinen, Lauri Anttila, and Mikko Valkama are with the Department of Electronics and Communications Engineering, Tampere University of Technology, Tampere, Finland.

Toni Lähteensuo is with Nokia Networks, Espoo, Finland.

Telecommunications-Advanced (IMT-Advanced), or the so-called 4G mobile systems. CA enables the aggregation of multiple LTE component carriers (CCs), that can have any bandwidth defined within the LTE specifications, while ensuring backwards compatibility with legacy LTE systems. It allows operators to flexibly aggregate the scattered spectral resources that lie in the same LTE band (intraband CA) or at different LTE bands (interband CA). Moreover, the aggregated carriers can have different bandwidths and may also be noncontiguously located even in the intraband case [1], [2], [5].

The flexibility of CA technology has several implications on the design and implementation of radio transceivers, in particular related to transceiver linearity requirements. While contiguous intraband CA and Release 8 single-carrier signals are still largely similar from the emissions perspective, the adoption of noncontiguous CA imposes significantly more stringent linearity requirements on the power amplifier (PA). This is because when excited with a noncongtinuous CA signal, the PA nonlinearities produce unwanted emissions that can interfere not only with the adjacent channels but also with more distant portions of the spectrum.

The levels of the unwanted emissions are generally controlled and regulated by the regional and international standardization bodies, in order to protect other devices and radio systems. In this context, the frequency division duplexing (FDD) mode of operation is generally more challenging, because transmitter emissions may leak into the RX chain, causing own receiver (self-)desensitization [12]-[15].

In general, a practical approach to meet the emission requirements as well as to relax the own RX desensitization problem is to reduce the transmit power level, such that the PA is operating in a more linear region. In 3GPP LTE/LTE-Advanced user equipment (UE) context, this is called maximum power reduction (MPR) [2]. However, reduced transmit power directly translates into reduced coverage and power efficiency. One specific solution for mitigating the RX desensitization problem is to improve the stopband attenuation of the duplexer filters, however, this will increase the passband insertion loss and duplexer cost. Therefore, it is imperative to explore solutions for meeting the required isolation between the TX and RX, while, at the same time, minimizing the insertion loss in order to improve the power efficiency and receiver sensitivity.

This article reviews the linearity requirements of LTE-Advanced mobile transmitters adopting CA waveforms, and the emissions and distortion resulting from nonlinear TX and RX components. A summary of uplink CA technology in different 3GPP releases is provided in Section II, together with an overview of alternative transmitter architectures. Then, the relevant emission limits and requirements of LTE-Advanced mobile terminals are discussed in details in Section III. We also identify the own receiver desensitization problem, stemming from the transmitter unwanted emissions. Motivated by this, we then review and demonstrate potential digital cancellation techniques with focus on intraband noncontiguous CA transmissions in order to relax the linearity and isolation requirements in FDD mobile transceivers in Section IV. The concluding remarks are made in the final section.

II. Uplink Carrier Aggregation Evolution and Candidate TX Architectures

A. Evolution of Uplink CA in LTE-Advanced

The evolution of CA in different 3GPP releases from the uplink perspective is summarized in this section, and is also illustrated graphically in Fig. 1(a). CA was originally introduced in 3GPP LTE-Advanced Release 10, and currently the RF specifications allow the aggregation of two UL CCs in intraband CA and up to three UL CCs in interband CA, in a limited number of cases [2][1]. The UL intraband contiguous CA with two CCs was introduced in Release 10, allowing contiguous and noncontiguous resource allocation within contiguously aggregated carriers to a UE. The noncontiguous resource allocation per CC or the so-called *multi-cluster transmission* was then introduced in Release 11 in order to improve uplink spectral efficiency. In Release 12, two major enhancements were introduced concerning noncontiguous CA (NC-CA): intraband NC-CA and interband CA. Intraband NC-CA allows non-adjacent carriers within an LTE band to be aggregated, thus giving more spectrum flexibility and enabling CA when contiguous carriers are not available. On the other hand, interband CA allows aggregating the CCs from more than one LTE band.

In addition, within Release 12, 3GPP has also specified the support for FDD-TDD CA. The aggregation of FDD and TDD carriers provides attractive benefits in terms of coverage and capacity. For example, in the uplink, a low band (LB) FDD carrier could be used for better coverage whereas a high band (HB) TDD carrier with more bandwidth could be used for achieving higher data rates. A new feature that is adopted in Release 13, to further boost the network capacity and data rates, is CA between an operator's licensed bands and unlincensed bands, known as licensed-assisted access (LAA). In LAA, the carrier in the licensed band coordinates the link, thus providing a reliable connection between the terminal and the base station (BS), while more bandwidth is opportunistically obtained from an unlicensed band.

B. Uplink Transmitter Architectures

To support wider bandwidths and fragmented spectrum, the baseline single-carrier (Release 8) transmitter architecture can be modified in several ways, as shown in Fig. 1(b). The complexity and challenges of these alternative transmitter architectures depend mainly on where the carriers are combined in the overall transmit chain. In principle, such carrier combining can take place either at the digital baseband or at the analog RF, with a common PA. Alternatively, all carriers can have independent PAs, after which the carriers are combined. The first architecture in Fig. 1(b) is feasible for the intraband contiguous CA cases where the CCs can easily be aggregated at the digital baseband and hence they can share the same mixer and PA. In the intraband NC-CA case, aggregation at the digital baseband results in an increased sample rate and complexity of digital-to-analog conversion (DAC). Furthermore, sharing a single mixer between different CCs may cause carrier leakage to fall onto a CC licensed to another operator,

[1]This applies to the RF specifications only. The baseband processing and network signaling specifications already allow up to 5 CCs since Release 10, while 3GPP is currently working on solutions with up to 32 CCs. Such large numbers of CCs will further complicate the RF design and performance, while in this paper we consider two UL CCs.

potentially violating the emission requirements. Therefore, typically each sub-block[2] is up-converted separately, as shown in the second architecture in Fig. 1(b), while the carriers still share a common PA.

The second architecture in Fig. 1(b) can also support interband CA, if the aggregated bands are closely spaced in frequency, by adopting a multi-band PA. However, if the aggregated bands are wide apart in frequency, such as aggregation of LB and HB carriers, then each LTE band typically has its dedicated transmitter chain and PA, and the LB and HB are combined through a diplexer, as illustrated in the third architecture in Fig. 1(b). The selectivity of the duplexers and diplexer helps better to isolate the PA outputs from each other, as compared to using a power combiner, which would also cause a substantial power loss. In general, in the context of intraband NC-CA and interband CA with CCs located in closely spaced frequency bands, the power efficiency of the overall transmitter is typically better with a single multi-band PA as compared to the multiple single-band PA-based architecture [6], since the power combining at the PA output is lossy and the efficiency of each single-band PA is typically low. However, the design of a multi-band PA is generally more complex, and the nonlinearity of a multi-band PA may result in severe intermodulation distortion (IMD), thus possibly requiring a large PA back-off.

III. LTE-Advanced Uplink Emission Limits and Transmitter Linearity Challenges

A. Transmit Signal Quality and Emission Requirements

In this section, 3GPP specifications for the transmitted signal quality of LTE/LTE-Advanced UE are reviewed and elaborated, with emphasis on the unwanted emissions outside the channel bandwidth.

The first performance metric to assess the quality of the transmitted signal is the *error vector magnitude* (EVM), which measures the error in the modulated signal constellation. The EVM is defined as the square-root ratio of the powers of the error signal and the clean signal component, and is typically expressed as a percentage ($\%$). It is generally evaluated after signal corrections such as symbol timing adjustment, carrier phase synchronization, DC offset removal, and equalization, and only the RBs allocated to a terminal are considered. The minimum requirements for EVM are that it shall not exceed 17.5% for QPSK and BPSK, 12.5% for $16-$QAM, and 8% for $64-$QAM modulation schemes [2], [3]. An additional requirement for LTE/LTE-Advanced terminals is the measure of *in-band emissions* from the allocated RBs falling into the non-allocated RBs within the channel bandwidth. The in-band emissions are measured as a ratio of emitted power at the non-allocated RBs located at a RB offset and the emitted power at the allocated RBs. As a result, the in-band emission limit specifies how much the transmission is allowed to interfere with non-allocated RBs that may potentially be allocated to other UEs.

The unwanted transmitter emissions outside the channel bandwidth are grouped into *out-of-band (OOB) emissions* and *spurious emissions*. OOB emissions refer to the emissions occurring immediately outside the desired channel bandwidth due to modulation process non-idealities and nonlinearity of the transmitter, however, excluding the spurious domain. On the other hand, the frequency range outside the channel bandwidth and the OOB emissions region is referred to as the spurious emissions domain.

[2]In NC-CA context, sub-block refers to a subset of contiguous CCs.

The OOB emissions are limited by *adjacent channel leakage ratio* (ACLR) and *spectrum emission mask* (SEM). ACLR quantifies the unwanted power that the transmitter emits within an adjacent channel, and is expressed as the power ratio between the wanted transmitted signal and the emissions onto an adjacent carrier. ACLR requirements in the 3GPP specifications for UE include three measurement scenarios: $\mathrm{UTRA}_{\mathrm{ACLR1}}$, $\mathrm{UTRA}_{\mathrm{ACLR2}}$, and $\mathrm{E-UTRA}_{\mathrm{ACLR}}$. $\mathrm{UTRA}_{\mathrm{ACLR1}}$ and $\mathrm{UTRA}_{\mathrm{ACLR2}}$ refer to two pairs of adjacent UTRA carriers on both sides of the transmitted E-UTRA (LTE) carrier, and this measurement is meant to protect the adjacent UMTS channels. Therefore, the power is measured using a UTRA receive filter with a measurement bandwidth of 3.84 MHz. In the OOB region, $\mathrm{E-UTRA}_{\mathrm{ACLR}}$ overlaps the $\mathrm{UTRA}_{\mathrm{ACLR1}}$ and $\mathrm{UTRA}_{\mathrm{ACLR2}}$ regions, and protects adjacent E-UTRA carriers. The measurement bandwidth of $\mathrm{E-UTRA}_{\mathrm{ACLR}}$ equals the channel bandwidth, excluding the guard bands. The minimum ACLR requirement for adjacent E-UTRA band is 30 dB, whereas for adjacent UTRA bands, the minimum requirements are 33 dB and 36 dB for $\mathrm{UTRA}_{\mathrm{ACLR1}}$ and $\mathrm{UTRA}_{\mathrm{ACLR2}}$, respectively [2], [3]. The measurement bandwidth of $\mathrm{CA\ E-UTRA}_{\mathrm{ACLR}}$ for intraband contiguous CA equals the aggregated channel bandwidth with guard bands excluded, i.e., $\mathrm{CA\ E-UTRA}_{\mathrm{ACLR}}$ treats the contiguously aggregated CCs as a single carrier. For NC-CA, the ACLR of each sub-block is defined similarly as described above for a sub-block, and the wanted channel power is the sum of channel powers of each sub-block. However, if the sub-block gap is too narrow to accommodate a channel protected by the ACLR limit, then the ACLR limit does not apply. For example, $\mathrm{UTRA}_{\mathrm{ACLR1}}$ is not measured if the sub-block gap is less than 5 MHz, whereas, if the sub-block gap is less than 15 MHz, $\mathrm{UTRA}_{\mathrm{ACLR2}}$ will not fit in and is thus not measured. Additionally, $\mathrm{CA\ E-UTRA}_{\mathrm{ACLR}}$ is not measured if it does not fit in the sub-block gap. Furthermore, $\mathrm{UTRA}_{\mathrm{ACLR2}}$ is omitted if it would overlap a $\mathrm{UTRA}_{\mathrm{ACLR1}}$ of another sub-block, however, $\mathrm{CA\ E-UTRA}_{\mathrm{ACLR}}$ measurement band is allowed to overlap another of its kind.

The SEM within the OOB region sets a limit for the maximum absolute leakage power to the adjacent channels. In general, the SEM is shaped to approximate the envelope of a typical spectral regrowth due to RF PA nonlinearity with full RB allocation, and is defined as piecewise constant expressed in terms of the power (in dBm) within a measurement bandwidth. In NC-CA, when OOB regions of sub-blocks overlap, the SEM section that corresponds to higher average power applies.

Spurious emissions are caused by the transmitter effects such as harmonic emissions, IMD products, parasitic emissions, and frequency conversion products, but exclude OOB emissions. The general spurious emissions limit for carrier frequencies greater than 1 GHz is -30 dBm within the measurement bandwidth of 1 MHz. However, in order to protect LTE bands against UE emission from other LTE bands, 3GPP specifies additional, stricter spurious emissions limits for coexistence. Furthermore, there can be additional SEM, ACLR, and spurious emissions requirements specified, e.g., to protect a certain LTE band in a particular geographical area. The UE is informed of any such additional requirements through network signaling.

The general emission limits and ACLR measurement regions for contiguous and noncontiguous CA transmissions are depicted in Fig. 2, together with example nonlinear PA output spectra assuming the transmit power level of $+23$ dBm. It can be seen from the figure that the emission limits can be easily fulfilled for contiguously aggregated carriers, however, the emissions in spurious domain are extremely challenging to manage particularly with narrow

TABLE I: MPR ranges in single CC and intraband CA transmission scenarios

CA mode	RB allocation	Max. MPR
Single CC	Contiguous	$\leq$ 2dB
	Noncontiguous	$\leq$ 8dB
Intraband contiguous CA	Contiguous	$\leq$ 3dB
	Noncontiguous	$\leq$ 8.5dB
Intraband noncontiguous CA		$\leq$ 18.5dB

noncontiguous resource allocations. Thus, a power back-off is needed to fulfill the emission requirements. In the following subsections, we elaborate in greater details on the challenges of employing noncontiguous transmissions and the needed power relaxation to meet the emission specifications.

B. Reduction of Unwanted Emissions Through MPR

The deployment flexibility of LTE-Advanced in terms of frequency resource allocation affects the nonlinear characteristics of the PA. Therefore, 3GPP has defined a relaxation of the maximum transmitted power that the UE must be able to produce, termed as *maximum power reduction* (MPR), which is usually applied when the PA would not otherwise be sufficiently linear for the transmitted waveform.

The MPR is determined as a function of one or few *feature variables* that are unique to the carriers configuration. These feature variables may include, e.g., the total number of RBs, the number of allocated RBs, and the distance of outermost cluster to the channel edges, etc. For noncontiguous resource allocations, the feature variable adopted by 3GPP is the *allocation ratio*, which is a ratio between the allocated RBs and the total number of RBs in the assigned CCs [2], [7]. In practice, MPR generally decreases when allocation ratio increases, as smaller allocation ratio imply high power spectral density at a given transmission power level, resulting in narrower but high spectral IMD products.

Table I summarizes the maximum MPR values for various transmission scenarios, assuming a common PA in all cases. It can be noticed that the maximum MPR values are small for contiguous RB allocations, as the PA nonlinearity-induced spectral regrowth does not reach far from the channel edges. However, the required MPR levels generally increase significantly with noncontiguous resource allocations and NC-CA transmission. The noncontiguous resource allocations destroy the single-carrier property of the uplink signal, and the PA nonlinearity creates multiple IMD products that may be located far from the carrier, possibly reaching the spurious emissions region. The worst case occurs when narrow clusters are allocated at the carrier edges. In the intraband NC-CA, the third-order IMD products most often fall in the spurious domain. This is because the width of the OOB region scales with the CC bandwidth rather than the total gross transmission bandwidth. Notice that in the interband CA case, the MPR requirements of a single CC apply for each carrier.

The baseline MPR specifications are independent of LTE operating bands. In certain frequency bands and geographical regions, where there are additional SEM, ACLR, and spurious emissions requirements to protect a

particular frequency band, *additional MPR* (A-MPR) can be granted through network deployment-specific signaling in order to meet stricter emission requirements [2], [3].

Finally, it is worth noting that while the MPR is an easy way to comply with the specified emission limits, it reduces the uplink coverage and throughput. Since noncontiguous allocations incur high MPR, the benefit of CA in the uplink may be compromised. The highest levels of MPR can often be avoided through proper radio resource management, i.e., by avoiding allocations that require high MPR. Also, power limited users that are typically close to the cell edges can be given priority to allocations with low MPR, such as single-CC with contiguous allocations, whereas other users operating close to the base station are not limited by higher MPRs. Furthermore, techniques such as PA linearization have the potential to reduce the needed MPR in the future [8].

IV. Own RX Desensitization and Digital Cancellation

A. TX-RX Nonlinearity-Induced RX Desensitization

In FDD transceivers, the adoption of CA tends to reduce the frequency separation between the coexisting UL and DL signals, particularly in NC-CA, as illustrated in Fig. 3(a). As a consequence, achieving sufficient TX-RX isolation through RF filtering becomes complicated[3], and the receiver can be exposed to the transmitter unwanted emissions. This can result in a phenomenon known as own RX desensitization or self-desensitization.

In the single CC and contiguous CA scenarios, the PA nonlinearity-induced spectral regrowth can extend into the receiver operating band, particularly in the case shown in Fig. 3(b), where the downlink secondary CC is located close to the uplink band. In NC-CA transmissions, the PA nonlinearity produces spurious IMD products of the CCs, which, in addition to causing spectral regrowth around the main carriers, appear at specific IM sub-bands that are at integer multiples of the inter-CC spacing. This is illustrated in Fig. 3(c) where a single PA is excited by a noncontiguous dual-carrier signal with carrier spacing of Δf. Some of these IM sub-bands can then lie at the own RX band, in particular if the duplex distance is close to an integer multiple of the carrier spacing, and may not be sufficiently suppressed by the duplexer TX filter [3], [4], as visualized conceptually in Fig. 3(d).

Similarly, on the receiver side, the presence of the TX in-band leakage signal imposes stringent linearity requirements on the RX front-end components, namely the mixers and the low noise amplifier (LNA). The nonlinearity of the mixer can generate second-order IMD (IMD2) due to the TX in-band leakage signal, that falls directly on top of the baseband downlink carrier, and is generally independent of duplex distance [9], [10], as shown in Fig. 3(e). On the other hand, the nonlinear distortion in the RX LNA produces IMD products of the TX in-band leakage signal which, in practice, coexist with the PA nonlinearity-induced IMD products and may cause additional self-interference to the downlink carriers.

In addition, the nonlinear distortion occurring in the passive components between the PA(s) and the antenna, such as switches, duplexers, and diplexers, can generate spurious IMD products that can fall on the receive band [3], [4], [11]. While the spurious IMD products generated by the active RF components are typically attenuated by

[3]This problem has been recognized by 3GPP, see, for example, 3GPP RAN Tdoc R4-123797, "UE Reference Sensitivity Requirements with Two UL Carriers," Ericsson and ST-Ericsson, Aug. 2012.

the duplexer, the passive IMD products experience only the insertion loss and may thus have considerable power compared to a weak received downlink signal.

B. Digital Cancellation of PA Nonlinearity-Induced Receiver Desensitization

To first demonstrate the receiver (self-)desensitization problem, we present a numerical example, assuming LTE uplink Band 25 and intraband noncontiguous CA transmission with CCs located at the edges of the uplink band. The effective duplex distance can then reduce to only 15 MHz. Then, the transmitter emissions leaking into the receiver chain can be up to -80 dBm/MHz[4], which is substantial when compared to the reference sensitivity level of the RX, typically between -101.2 dBm/1.08 MHz to -90.5 dBm/18 MHz for the 1.4 MHz and 20 MHz channels, respectively, and thus fully desensitize the receiver.

The approach adopted by 3GPP to cope with this problem is to permit a certain amount of self-desensitization when TX emissions fall onto the receiver band in noncontiguous CA transmissions. This is done through relaxing the reference sensitivity requirements by an amount known as *maximum sensitivity degradation* (MSD) when UE transmits at the maximum power [2], [3]. This approach is, however, not very appealing nor practical for the power limited weak users. Instead of resorting to these conventional solutions, such as the MSD or the ones we discussed already in the Introduction section, we discuss in this article the potential of adopting digital cancellation techniques to relax the RX self-desensitization problem.

The fundamental idea behind the digital cancellation techniques is to create a replica of the self-interference in the transceivers digital front-end, through sophisticated nonlinear signal processing, and then subtract the regenerated self-interference from the received signal, such that the overall interference at the RX band is suppressed. Among digital cancellation techniques reported in the recent literature to resolve the RX desensitization problem, the techniques proposed in [12] and [13] can, in general, be adopted in both contiguous and NC-CA transmission cases. However, they treat the multi-CC waveform as a single wideband signal, and thus the associated computational complexity may become very high. To reduce the complexity, sub-band interference regeneration and cancellation techniques have recently been proposed in [14], [15], where modeling and cancellation of the self-interference at the specific IM sub-bands that are located in the RX band is pursued. In [12] and [14], the assumed PA model is memoryless, and further simplifying assumptions in the basis functions generation are made in [14], which will limit the obtainable cancellation performance with these techniques. In [13] and [15], on the other hand, more accurate overall modeling, including PA model with memory and arbitrary frequency-selective duplexer response, is utilized, enabling efficient estimation and cancellation of the nonlinear self-interference at the RX band.

Fig. 4 illustrates a conceptual CA FDD transceiver block diagram incorporating the overall digital interference regeneration and cancellation unit. The *configuration unit* drives the interference cancellation unit whose parameters depend on the transmitted waveform characteristics, and can flexibly activate and deactivate one or several inter-

[4]The spurious emissions at the RX band, evaluated at the antenna interface, are assumed to meet the general spurious emissions limit for LTE/LTE-Advanced UEs, i.e., -30 dBm/MHz, being then further suppressed by the duplexer filter, with an assumed isolation of 50 dB.

ference regeneration and cancellation blocks. Detailed technical descriptions of the alternative digital cancellation solutions can be found in [12] - [15].

C. Simulation and RF Measurement Examples

The performance of the aforementioned digital cancellation schemes is demonstrated in this subsection through MATLAB simulations and true RF measurements, by quantifying the obtained interference suppression and evaluating the receiver signal-to-interference plus noise ratio (SINR) against different transmit power levels.

The impact of TX unwanted emissions extending into the RX band, and its digital cancellation, is first investigated through simulations. We assume a scenario with a single uplink and two downlink CCs, as shown in Fig. 3(b). The TX signal, namely a fully-allocated single-carrier 10 MHz LTE-Advanced uplink signal, is applied to a wideband Wiener PA model of nonlinearity order 5 with PA gain, IIP3, and output 1 dB compression point equal to 20 dB, $+17$ dBm, and $+27$ dBm, respectively. The PA model is extracted from a real mobile PA. The TX power is $+23$ dBm. The duplexer TX and RX filters are based on measurements of a real mobile duplexer, and have $50-60$ dB isolation. To reflect a challenging scenario, the duplex distance is assumed to be only 15 MHz. The desired RX signal is a dual-carrier NC-CA LTE-Advanced downlink signal, with 10 MHz CCs each operating 10 dB above the reference sensitivity level, i.e., -83.5 dBm [2]. Fig. 5(a) shows the simulated RX input referred power spectra of different signal components at the RX band of DL CC1, showing clearly that the TX emissions leaking into the RX band are quite substantial, thus heavily corrupting the reception of the close-in downlink carrier. The digital cancellation technique [13] creates a replica of the nonlinear self-interference leaking into the RX band, by first estimating the unknown responses of the duplexer filters and the nonlinear PA with memory, and then using the known transmit data as reference for the self-interference regeneration. The generated TX leakage signal replica is then subtracted from the received signal, to suppress the overall interference at the RX band. It can be observed that the digital cancellation technique is able to efficiently push the self-interference below the thermal noise floor within the carrier bandwidth. The performance is further quantified by plotting the average SINR of the downlink CC affected by TX emissions with different power levels, and the obtained curves are shown in Fig. 5(b). Here, the detrimental impact of the self-interference on the RX performance can be seen more clearly; nevertheless, the digital cancellation technique is able to suppress it and clearly enhance the RX SINR.

Next, we report true RF measurement results carried out using commercial LTE Band 25 (UL: $1850-1915$ MHz, DL: $1930-1995$ MHz) PA and duplexer modules for UE FDD transceivers. The baseband TX signal is now a dual-carrier LTE-Advanced uplink signal with fully-allocated 5 MHz CCs and 35 MHz sub-block gap, being generated locally on the computer, and the samples are transferred to the National Instruments (NI) vector signal transceiver (VST), which performs I/Q up-conversion at 1880 MHz. The VST output signal drives the PA module, whose output is then fed to the duplexer TX port. In such a noncontiguous carrier configuration, the duplex gap reduces to 40 MHz, and the positive IM3 sub-band is located at 1940 MHz, which is also the operating band of the downlink CC. The desired RX signal, also a dual-carrier LTE-Advanced downlink signal, is assumed to be operating 10 dB above the reference sensitivity level. The desired RX signal is generated by a vector signal generator (VSG)

and is injected to the antenna port of the duplexer. The duplexer RX port is connected to VST, which also performs IQ down-conversion and digitization of the received signal.

The required MPR for the given PA module is first determined to be 10 dB in order to reach the spurious emissions limit of -30 dBm/MHz, which corresponds to $+13$ dBm TX power. This is well inline with 3GPP specifications, which allow 12 dB MPR, and thus $+11$ dBm TX power, with the assumed CC bandwidths [2]. At $+13$ dBm TX power, the measured baseband spurious IMD interference at the RX band, referred to the RX input, is shown in Fig. 5(c). It is evident that even though the spurious emissions limit is satisfied, the self-interference at the RX band is still substantial, and is in fact blocking the reception as it seriously masks the desired RX CC. We then employ the digital sub-band interference regeneration and cancellation technique, based on an extension of [15], considering now up to eleventh-order IMD products at the IM3+ sub-band. The considered technique, operating in the transceiver digital front-end, estimates the unknown responses of the duplexer filters and the nonlinear PA with memory at the specific IM3 sub-band, and subsequently regenerates and cancels the self-interference. It can be observed from the PSD curves in Fig. 5(c) that the sub-band digital cancellation technique is able to suppress the interference close to the system noise floor. In the final experiment, we perform SINR measurements for different transmit powers with no MPR, and the measured SINR curves are plotted in Fig. 5(d). The obtained curves show that spurious IM3 self-interference severely affects the RX performance even at lower transmission powers, while the digital cancellation technique can clearly enhance the RX SINR. The digital cancellation at best gives up to 21 dB of self-interference suppression, and extends the usable transmit power range by about 8 dB, when allowing a 1 dB drop in the SINR.

V. Conclusion

In this article, an overview of the linearity requirements and challenges of LTE-Advanced mobile transmitters was presented, with emphasis on PA-induced spurious emissions at own RX band and their mitigation through digital cancellation in simultaneous transmit and receive systems. The evolution of uplink CA in different LTE releases, and the corresponding transmitter architectures for different CA modes were first reviewed. It was concluded that the noncontiguous transmissions cause serious nonlinear distortion in the TX, in particular due to PA nonlinearity, and require a considerable PA back-off to reach the emission limits. Furthermore, the nonlinearities of the TX chain can also cause spurious distortion at the own RX band that may lead to RX desensitization. To prevent this, a nonlinear self-interference regeneration and cancellation architecture was then reviewed. The simulation and RF measurement results demonstrate that excellent suppression of the self-interference can be achieved by adopting digital cancellation techniques. Such digital cancellation solutions are likely to be one key enabling technology for increased flexibility and efficiency in the RF spectrum utilization, in the future LTE-Advanced and 5G networks.

Acknowledgments

This work was supported by the Academy of Finland, under the projects #284694, #288670, #301820, #304147, Nokia Networks, Finland, and Nokia Bell Labs, Finland.

REFERENCES

[1] E. Dahlman, S. Parkvall, and J. Sköld, *4G: LTE/LTE-Advanced for Mobile Broadband,* Elsevier, 2011.

[2] 3GPP TS 36.101, "User Equipment (UE) Radio Transmission and Reception," Ver. 13.5.0, Release 13, Sept. 2016.

[3] 3GPP TS 36.521, "User Equipment (UE) Conformance Specification Radio Transmission and Reception," Ver. 14.0.0, Release 14, Sept. 2016.

[4] 3GPP TR 36.860, "LTE Advanced Dual Uplink Inter-band Carrier Aggregation," Ver. 1.0.0, Release 12, Dec. 2014.

[5] C. S. Park, L. Sundström, A. Wallen, and A. Khayrallah, "Carrier Aggregation for LTE-Advanced: Design Challenges of Terminals," *IEEE Commun. Mag.*, vol. 51, no. 12, Dec. 2013, pp. 76-84.

[6] S. A. Bassam *et al.*, "Transmitter Architecture for CA: Carrier Aggregation in LTE-Advanced Systems," *IEEE Microw. Mag.*, vol. 14, no. 5, July-Aug. 2013, pp. 78-86.

[7] V. Lehtinen *et al.*,, "Gating Factor Analysis of Maximum Power Reduction in Multicluster LTE-A Uplink Transmission," Proc. *IEEE RWS,* 2013, pp. 151-153.

[8] M. Abdelaziz *et al.*,, "Digital Predistortion for Mitigating Spurious Emissions in Spectrally Agile Radios," *IEEE Commun. Mag.*, vol. 54, no. 3, Mar. 2016, pp. 60-69.

[9] A. Kiayani *et al.*, "Modeling and Dynamic Cancellation of TX-RX Leakage in FDD Transceivers," Proc. *IEEE MWSCAS*, 2013, pp. 1089-1094.

[10] A. Frotzscher and G. Fettweis, "Digital Compensation of Transmitter Leakage in FDD Zero-IF Receivers," *Trans. Emerging Tel. Tech.,* vol. 23, no. 2, Mar. 2012, pp. 105-120.

[11] H. -T. Dabag *et al.*, "All-Digital Cancellation Technique to Mitigate Receiver Desensitization in Uplink Carrier Aggregation in Cellular Handsets," *IEEE Trans. Microw. Theory Techn.,* vol. 61, no. 12, Dec. 2013, pp. 4754-4765.

[12] M. Omer *et al.*, "A Compensation Scheme to Allow Full Duplex Operation in the Presence of Highly Nonlinear Microwave Components for 4G Systems,"' Proc. *IEEE MTT-S Intl. Microw. Symp.*, 2011, pp. 1-4.

[13] A. Kiayani *et al.*, "Digital Suppression of Power Amplifier Spurious Emissions at Receiver Band in FDD Transceivers,"' *IEEE Signal Process. Lett.,* vol. 21, no. 1, Jan. 2014, pp. 69-73.

[14] C. Yu *et al.*, "Digital Compensation for Transmitter Leakage in Non-Contiguous Carrier Aggregation Applications with FPGA Implementation," *IEEE Trans. Microw. Theory Techn.,* vol. 64, no. 12, Dec. 2015, pp. 4706-4318.

[15] A. Kiayani *et al.*, "Digital Mitigation of Transmitter-Induced Receiver Desensitization in Carrier Aggregation FDD Transceivers," *IEEE Trans. Microw. Theory Techn.,* vol. 63, no. 11, Dec. 2015, pp. 3608-3623.

PLACE
PHOTO
HERE

Adnan Kiayani (adnan.kiayani@tut.fi) received his B.Sc. degree from COMSATS Institute of Information Technology, Pakistan, the M. Sc. (with honors) and Dr. Tech. degrees from Tampere University of Technology (TUT), Finland, in 2006, 2009 and 2015, all in electrical engineering. Currently, he is a post-doctoral researcher at the Department of Electronics and Communications Engineering at TUT. His general research interests are in signal processing for communications, and is currently working on digital and RF cancellation techniques for self-interference suppression in simultaneous transmit and receive systems.

PLACE
PHOTO
HERE

Vesa Lehtinen (vesa.lehtinen@tut.fi) received the Diploma Engineer degree from the Tampere University of Technology (TUT), Tampere, Finland, in 2003, and is currently working towards the Ph.D. degree at TUT. His research interests include linear multirate filtering and sampling techniques, as well as analysis and mitigation of radio transceiver front-end non-idealities.

PLACE
PHOTO
HERE

Lauri Anttila (lauri.anttila@tut.fi) received the M.Sc. degree and D.Sc. (Tech) degree (with honors) in electrical engineering from Tampere University of Technology (TUT), Tampere, Finland, in 2004 and 2011. Currently, he is a Senior Research Fellow at the Department of Electronics and Communications Engineering at TUT. His research interests are in signal processing for wireless communications, radio implementation challenges in 5G cellular radio and full-duplex radio, flexible duplexing techniques, and transmitter and receiver linearization. He has co-authored over 70 peer reviewed articles in these areas, as well as two book chapters.

PLACE
PHOTO
HERE

Toni Lähteensuo (toni.h.lahteensuo@nokia.com) was born in Eura, Finland, on August 22nd, 1988. He received the M.Sc. degree in electrical engineering in 2013 from Tampere University of Technology (TUT), Tampere, Finland. He has been working in radio access system research, standardization and implementation related projects at Nokia and Nokia Networks since 2013.

PLACE
PHOTO
HERE

Mikko Valkama (mikko.e.valkama@tut.fi) received his M.Sc. and Ph.D. degrees (both with honors) in electrical engineering from Tampere University of Technology (TUT), Finland, in 2000 and 2001, respectively. Currently, he is a Full Professor and Department Vice-head at the Department of Electronics and Communications Engineering at TUT. His general research interests include communications signal processing, estimation and detection techniques, signal processing algorithms for flexible radio transmitters and receivers, cognitive radio, full-duplex radio, radio localization, 5G mobile cellular radio networks, digital transmission techniques such as different variants of multicarrier modulation methods and OFDM, and radio resource management for ad hoc and mobile networks.

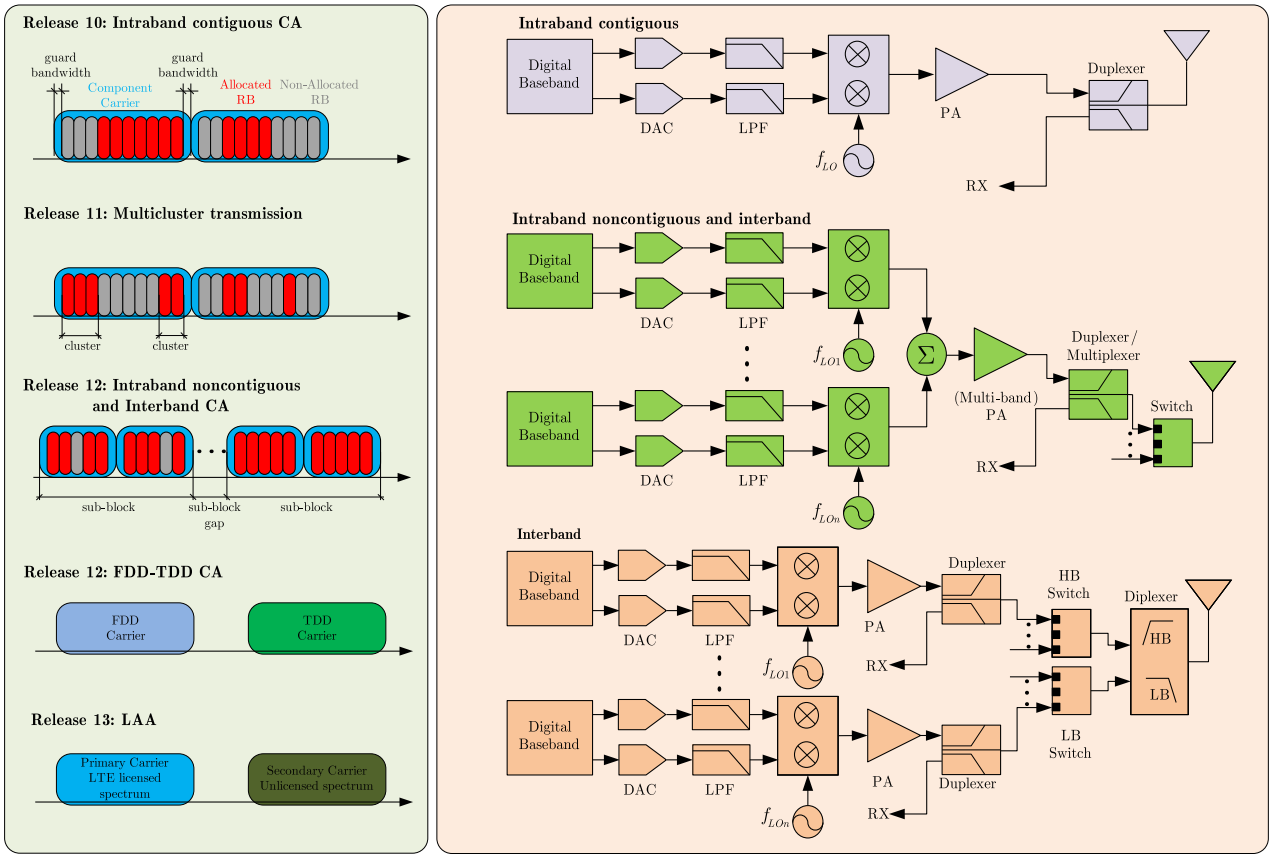

(a) (b)

Fig. 1: Uplink carrier aggregation in LTE-Advanced with two UL CCs: (a) different types of CA schemes in LTE-Advanced uplink from a single user perspective; (b) transmitter architectures suitable for different CA variants.

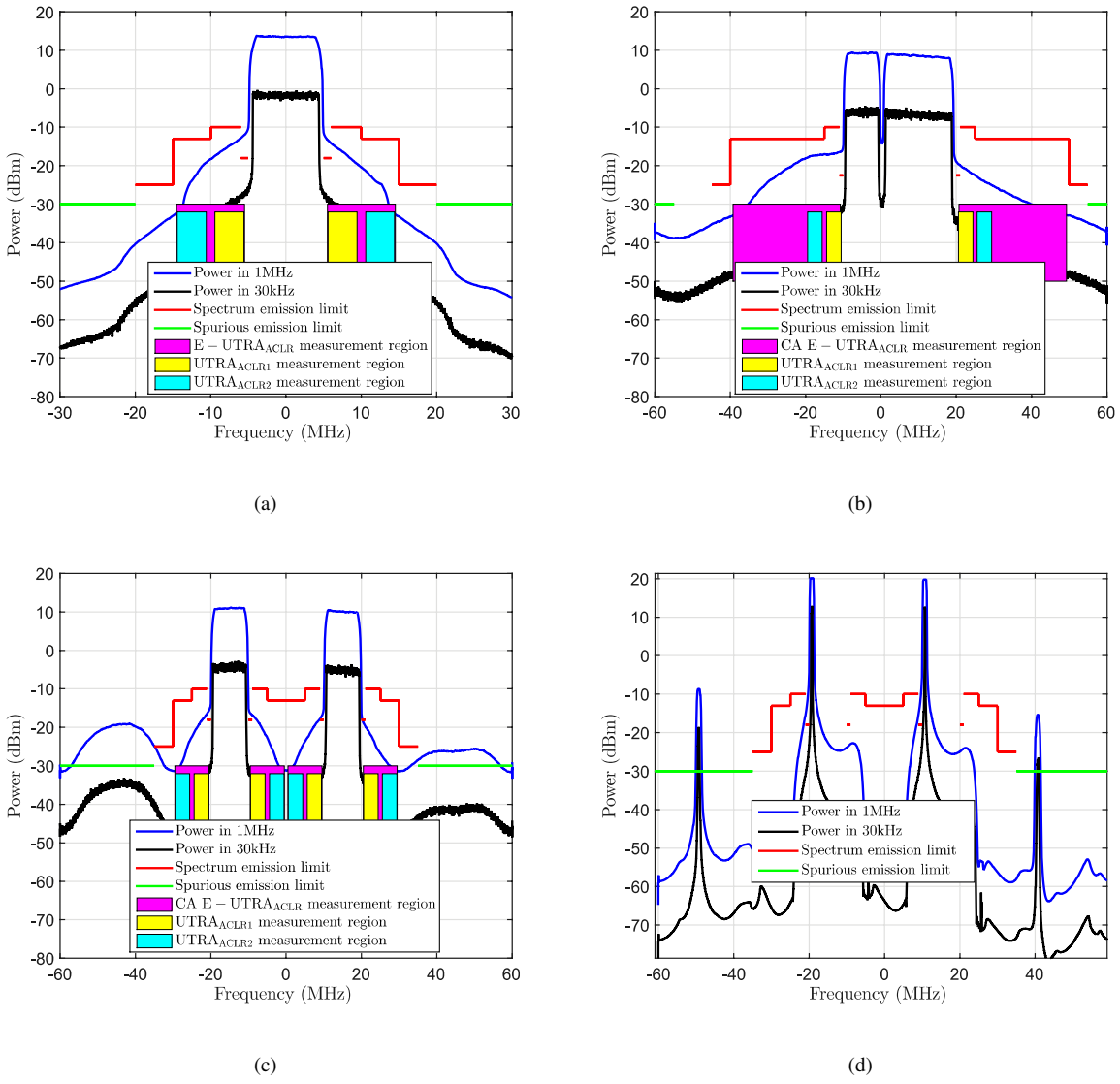

Fig. 2: Spectrum emission limits and ACLR measurement regions for LTE-Advanced mobile transmitters. Simulated examples showing baseband equivalent spectra assuming a common PA and +23 dBm transmit power: (a) single fully allocated 10 MHz carrier; (b) contiguous CA with fully allocated 10 MHz and 20 MHz CCs; (b) intraband noncontiguous CA with two fully allocated 10 MHz CCs and 20 MHz sub-block gap; (d) intraband noncontiguous CA with two CCs each allocated 1 RB and 20 MHz sub-block gap.

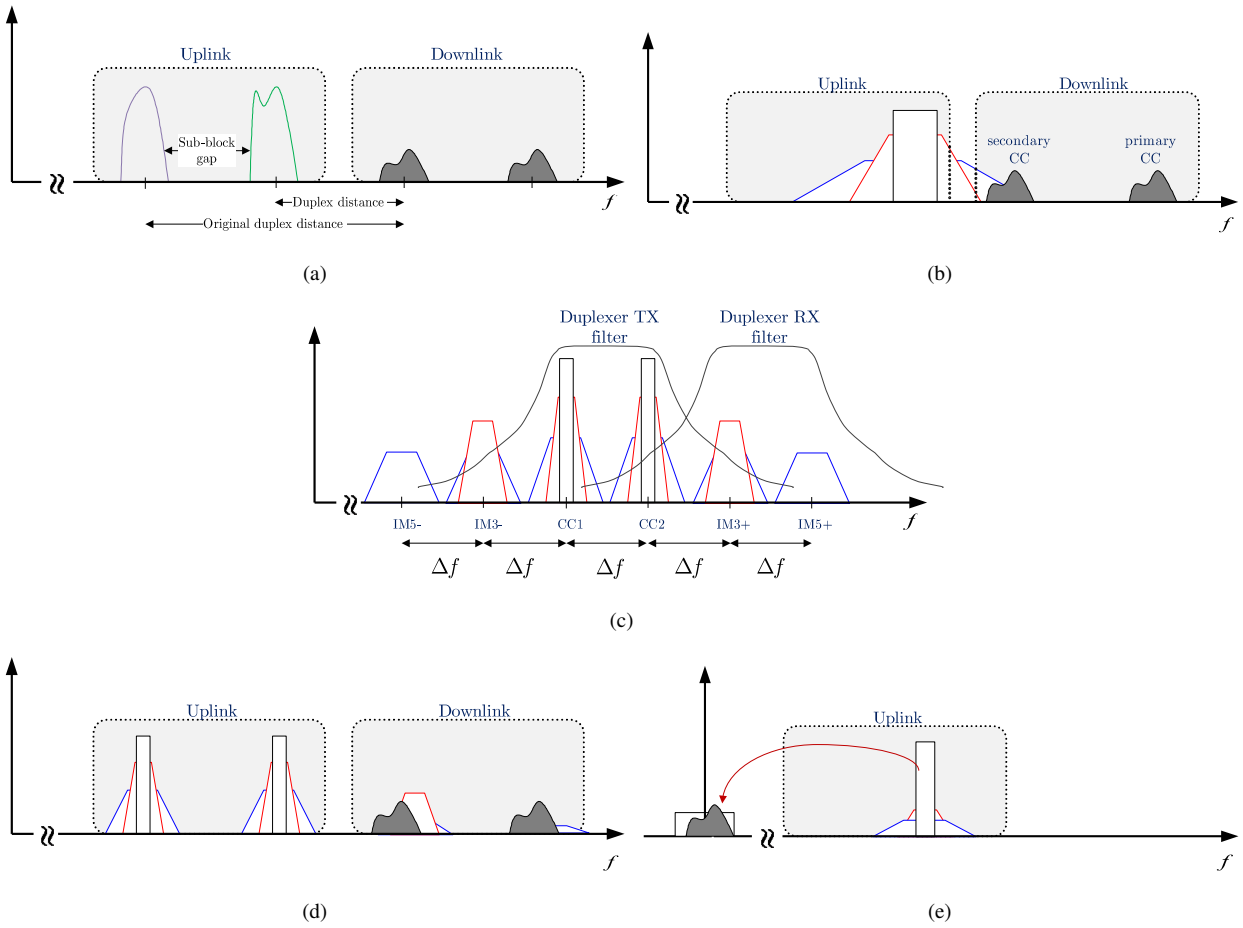

Fig. 3: Example spectral illustrations with contiguous and noncontiguous CA transmission under nonlinear TX and RX chain components and finite duplexer isolation: (a) impact of sub-block gap on the original duplex distance; (b) TX emissions extending into the RX band with single uplink carrier and two downlink carriers; (c) spurious IMD products created by either a nonlinear TX PA or nonlinear RX LNA with a noncontiguous dual-carrier signal; (d) spurious IMD products in the own RX band created by nonlinear TX-RX chain components, causing interference to downlink carriers; (e) TX in-band leakage signal induced spurious IMD2 due to a nonlinear mixer in the RX chain.

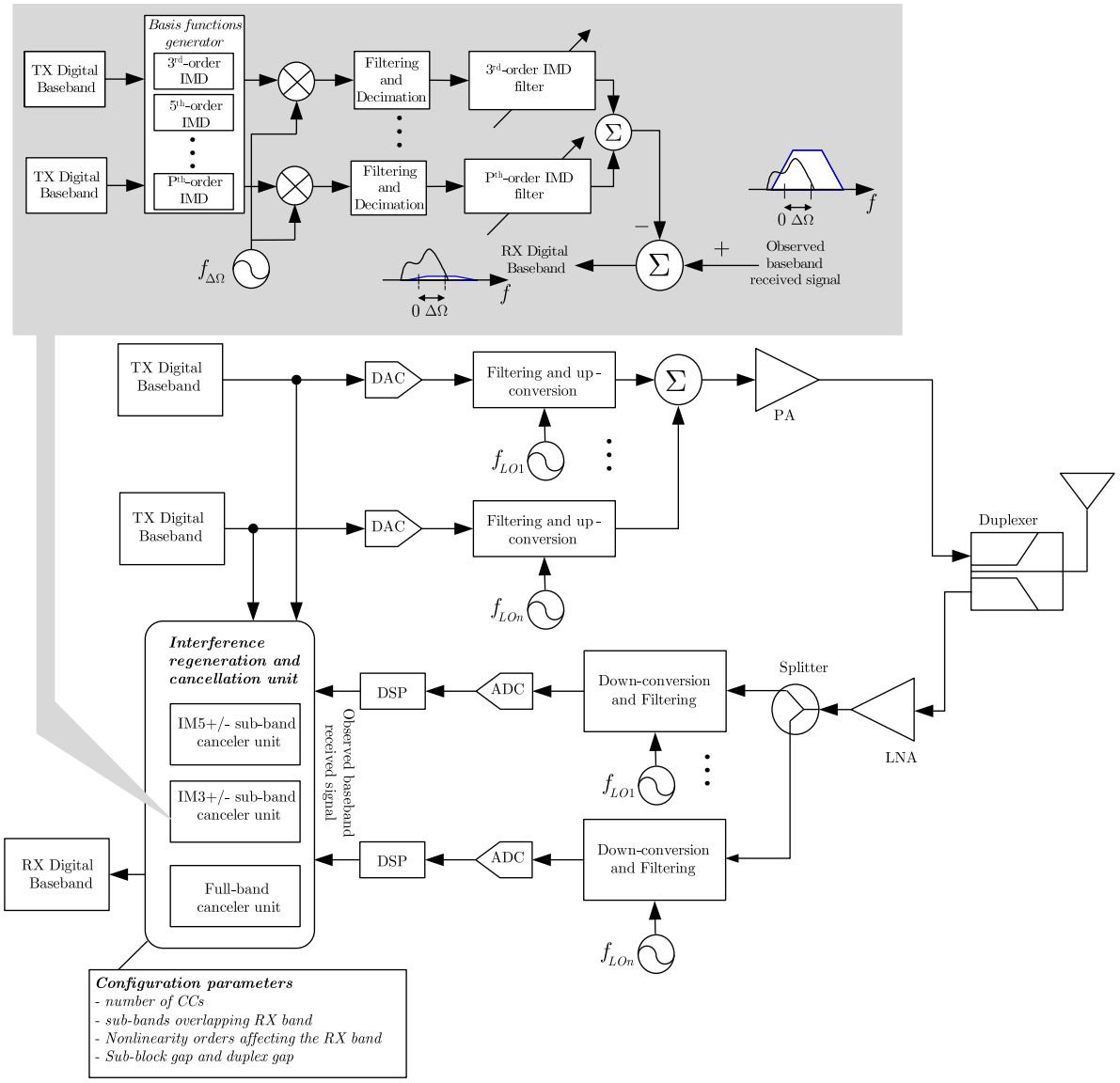

Fig. 4: A detailed block diagram of an intraband CA FDD transceiver adopting digital interference regeneration and cancellation unit to suppress the PA nonlinearity-induced self-interference at the own RX band. The cancellation units can be flexibly activated or de-activated depending on the input from the configuration unit. As an example, the architecture of self-interference regeneration and cancellation unit operating at positive IM3 (IM3+) sub-band is shown in detail on the top, assuming intraband noncontiguous CA with two CCs and considering up to $P^{th}-$order IMD at IM3+ sub-band.

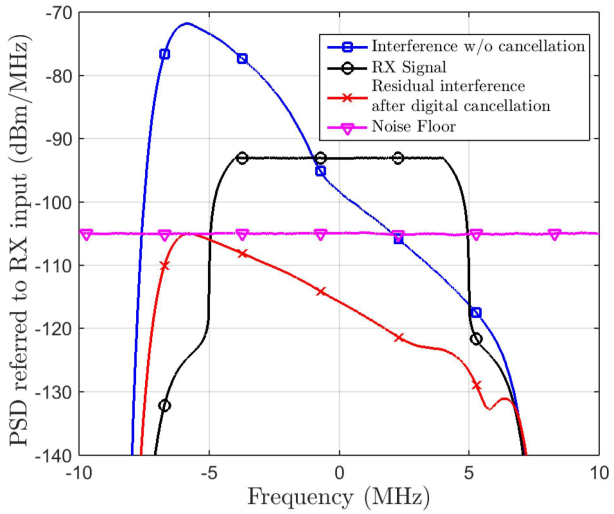

TX signal: 10 MHz LTE UL signal;
RX signal: dual-carrier noncontiguous LTE DL signal, 10MHz per CC;
TX power: +23 dBm; MPR/A-MPR: 0 dB; Duplex distance: 15 MHz;
RX power: -83.5 dBm; RX NF: 9 dB; Duplexer isolation: 50-60 dB

(a)

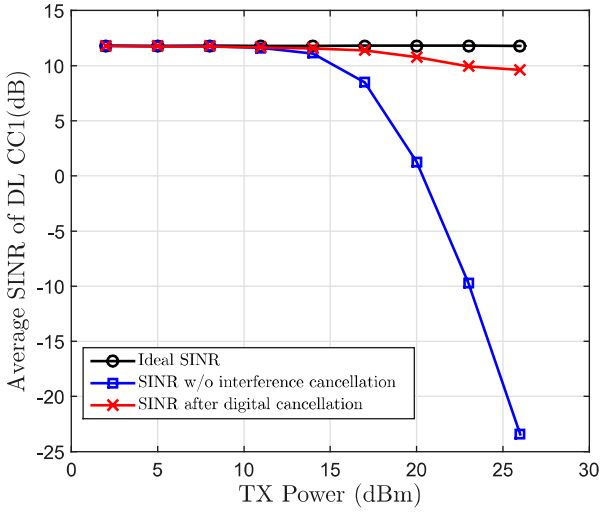

TX signal: 10 MHz LTE UL signal;
RX signal: dual-carrier noncontiguous LTE DL signal, 10MHz per CC;
TX power: [0 - 23] dBm; MPR/A-MPR: 0 dB; Duplex distance: 15 MHz;
RX power: -83.5 dBm; RX NF: 9 dB; Duplexer isolation: 50-60 dB

(b)

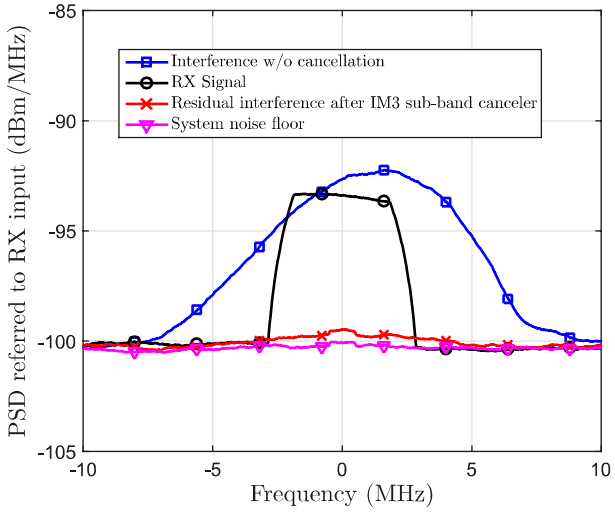

TX signal: dual-carrier noncontiguous CA LTE UL signal, 5 MHz per CC,
35 MHz sub-block gap; RX signal: LTE DL signal, 5MHz per CC;
TX power: +14 dBm; MPR/A-MPR: 9 dB; Duplex distance: 40 MHz;
RX power: -86.5 dBm; RX NF: 14 dB; Duplexer isolation: 55-60 dB

(c)

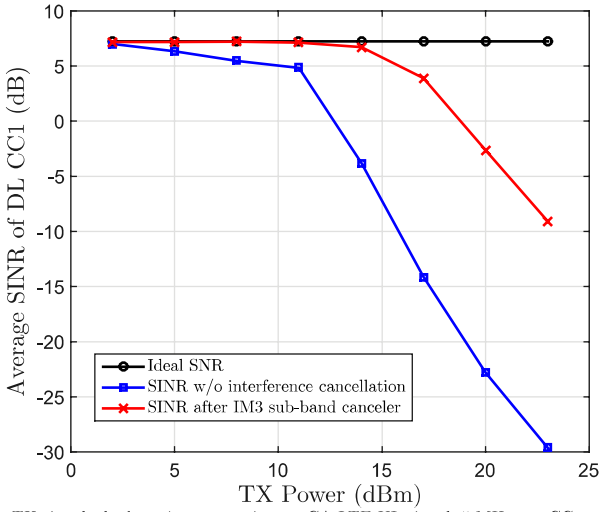

TX signal: dual-carrier noncontiguous CA LTE UL signal, 5 MHz per CC,
35 MHz sub-block gap; RX signal: LTE DL signal, 5MHz per CC;
TX power: [0 - 23] dBm; No MPR/A-MPR; Duplex distance: 40 MHz;
RX power: -86.5 dBm; RX NF: 14 dB; Duplexer isolation: 55-60 dB

(d)

Fig. 5: Digital mitigation of own RX desensitization in CA FDD transceivers: (a) simulated power spectra of the transmitter emissions leaking into the RX band of the close-in DL CC before and after digital cancellation, the desired RX signal, and the thermal noise; (b) simulated RX SINR of the close-in DL CC against different transmit power levels, before and after the digital cancellation; (c) measured power spectra of the self-interference at spurious positive IM3 sub-band in noncontiguous CA transmission scenario before and after digital cancellation, the desired RX signal, and the system noise floor; (d) measured own RX SINR versus transmit powers, before and after the digital cancellation.